Theory of Brillouin scattering from opaque media

N. L. Rowell and G. I. Stegeman
Department of Physics, University of Toronto, Toronto, Canada M5S 1A7
(Received 11 April 1978)

The general theory of Brillouin scattering from the surfaces of opaque media is developed using a total field solution approach. Acoustical modes appropriate to a stress-free surface are found from solutions to the acoustical-wave equation and boundary conditions for a finite isotropic medium. Two light-scattering mechanisms, namely, the surface corrugation and bulk elasto-optical effects, were analyzed by deriving optical fields which satisfy both the acousto-optically driven wave equation and the electromagnetic boundary conditions. The special case for a metal of scattering by acoustically created conductivity fluctuations was also investigated in a similar way. The Brillouin spectrum was obtained by summing the scattering from the individual acoustical modes over the density of phonon states. Excellent agreement was obtained with experiment for Brillouin scattering from the metals gallium (liquid) and aluminum (solid).

I. INTRODUCTION

Brillouin scattering from thermal phonons in bulk media has been utilized extensively to study transparent solids and liquids.[1-6] The most recent developments in this field deal with scattering from thermal phonons at the surfaces of opaque[7-9] and transparent materials.[10-12] These experiments are technically very difficult due to the intense stray light scattering which occurs at imperfect surfaces. This phenomenon is characterized by penetration depths of one wavelength or less for the incident light with the result that the wave-vector component normal to the surface is not conserved in the acousto-optical interaction. Therefore for a specific scattering direction the frequency spectrum is relatively broad since the scattering takes place from phonons of a continuum of wave vectors rather than from phonons of a discrete wave vector as occurs in the Brillouin spectrum of bulk media. It then becomes necessary to have a detailed theory of the phenomenon in order to deduce accurate acoustical information from the spectra.

The first two papers on Brillouin scattering from opaque materials by Bennett and Maradudin,[13] and by Sandercock[7] were of a theoretical and experimental nature, respectively. Bennett and Maradudin analyzed the elasto-optical effect within the skin depth of aluminum and concluded that experiments on metals were feasible. Sandercock reported backscattering measurements on semiconductor surfaces. In the same year Sandercock[10] also measured the Brillouin spectrum of a free-standing film. The first experiments on metals (liquid) were reported in 1976 by Dil and Brody.[8] These authors were unsuccessful in interpreting their spectra in terms of scattering from acoustically induced electron-density fluctuations in the metallic free-electron gas, within the skin depth. Dervisch and Loudon[14] and Dresselhaus and Pine[15] identified the appropriate acoustical modes as those of a semi-infinite rather than an infinite medium. In 1976 we reported[11] the Brillouin spectra of thin films deposited on substrates. Excellent agreement was obtained between experiment and theory by using the acoustical modes appropriate to the surface of a semi-infinite medium and by treating light scattering from both the elasto-optical and corrugation mechanisms. The theory was subsequently refined[12] by deriving the normal modes of a thin film on a semi-infinite medium. Very recently Sandercock[9] has measured the Brillouin spectrum from solid metal surfaces and found that the spectra were not described adequately by previous theories.[13,14] Loudon[16] has interpreted the frequency spectra and has shown that the primary scattering mechanism is the corrugation produced at the surface by the phonons. Independently we[17] extended our formalism to the analysis of Brillouin scattering from metals and interpreted the results of Dil and Brody[8] on liquid metals as well as those of Sandercock[9] on aluminum utilizing both the corrugation and conductivity mechanisms. In this paper we present the details of our calculations and also treat the elasto-optical effect in order to complete the theory.

The problem of Brillouin scattering at surfaces requires the analysis of (a) the acoustical modes at a surface and their density of states, (b) the acousto-optical interaction, and (c) the Brillouin spectrum.

The acoustical modes are those appropriate to a semi-infinite medium or a thick plate. The key point is that the surface(s) must be stress free which leads to a mixing of the sound modes associated with an infinite medium. In a liquid, only longitudinal modes are considered and a standing wave is formed which results in a stress-free surface. (The possibility of coupling to a shear type of mode at the surface is considered in the Appendix.) In a solid the resulting normal modes consist of surface phonons and linear combinations of standing waves of the usual shear and longitudinal phonons. The analysis in this paper is based on finding total field solutions of the acoustical-wave equations which also satisfy the boundary conditions. (It is also possible to use Green's functions[18] to evaluate these fields.) These aspects of the calculation are discussed in Secs. II–IV.

Two scattering mechanisms, namely the corrugation and elasto-optical effects, are considered. Scattering via the corrugation effect[19-22] from generated surface and bulk acoustical waves is well known. The corrugation acts as a traveling diffraction grating and Doppler shifted light is scattered into diffraction "orders." A general theory for this phenomenon for surface waves on dielectric media is available[23] and was extended here to opaque media. The elasto-optical effect was treated by solving for the total fields which satisfy the driven wave equation and electromagnetic boundary conditions. A special case, that of conductivity fluctuations in an electron gas, was analyzed separately using the same technique. The result of Secs. V–VIII is an expression for the field scattered by a single acoustical mode.

The Brillouin spectrum from each acoustical mode is calculated in a standard way, i.e., from the electric field correlation function. The complete spectrum is calculated by summing the individual mode contributions over the density of states (Sec. IX). The analytical expressions are evaluated for liquid and solid metals and are compared with previously reported experiments in Sec. X. The principal results of this paper are summarized in Sec. XI.

II. ACOUSTICAL MODES – GENERAL

The equations which govern the propagation of phonons in any medium are well known.[24] The mechanical displacement $\vec{u}$ associated with a sound wave satisfies the acoustical wave equation (force balance)

$$\nabla_i T_{ij} = \rho \ddot{u}_j . \tag{1}$$

Here T_{ij} is the stress (force per unit area) and ρ the mass density. For a solid and a liquid

$$T_{ij} = \tfrac{1}{2} c_{ijkl} \left(\frac{\partial u_k}{\partial x_l} + \frac{\partial u_l}{\partial x_k} \right) \tag{2}$$

and

$$T_{ij} = \rho v_L^2 \frac{\partial u_i}{\partial x_j} \delta_{ij} + \eta \left(\frac{\partial \dot{u}_i}{\partial x_j} + \frac{\partial \dot{u}_j}{\partial x_i} \right), \tag{3}$$

respectively, where c_{ijkl} are the second-order elastic constants, v_L is the longitudinal wave velocity in the liquid, and η is the fluid shear viscosity. In infinite media, the solutions for liquids consist of longitudinal waves ($\vec{\nabla} \times \vec{u} = 0$) (for small η) and for solids, they consist of longitudinal and transverse waves.

The existence of a free boundary introduces stress-free boundary conditions at the surface, i.e., $T_{zj} = 0$ for an interface in the x-y plane. A sound wave incident on a surface gives rise to[23] reflected waves of the same or of different polarization. For example, in a semi-infinite solid an incident shear wave polarized out of the plane of the surface produces a reflected shear wave and either a propagating or an evanescent longitudinal wave. There are two quantities which are conserved in this process, i.e., the frequency Ω and $\vec{q}_\parallel$, the component of the wave vectors parallel to the surface. Thus normal modes at a surface are characterized by $\vec{q}_\parallel$ and Ω, rather than the total wave vector $\vec{q}$ which is the case for infinite media. Furthermore, we note that the normal modes excited by thermal fluctuations are basically standing waves. Therefore the normal modes near a surface consist of linear superpositions[25] of standing-wave shear and longitudinal phonons characterized by equal values of $\vec{q}_\parallel$ and Ω. Since there are three orthogonal solutions allowed by the wave equation, there exist three orthogonal modes for a given value of Ω and $\vec{q}_\parallel$.

The analysis of the acoustical modes proceeds along classical lines.[24] Since most Brillouin-scattering experiments are performed at flat surfaces, the medium is modeled as a flat plate of area A and thickness $2L_z$ (as shown in Fig. 1). Only isotropic media are considered, and the phonon wave vectors are assumed to lie in the x-z plane. In such a flat-plate geometry, one surface is sufficient to derive the form of the normal modes. The appropriate density of states is taken from the work of Stratton,[26] when necessary.

III. ACOUSTICAL MODES – LIQUIDS

The normal modes of a bounded liquid, their normalization to the energy provided by thermal

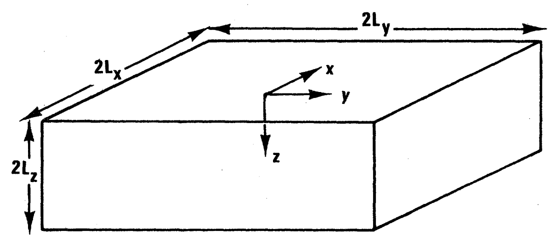

FIG. 1. Geometry for the analysis of the acoustical modes of a thick plate.

fluctuations and their density of states are discussed in this section.

A liquid can support longitudinal waves at all frequencies as well as shear waves at high frequencies for some viscous liquids.[3] Of interest in this paper are metallic liquids such as mercury and gallium and for frequencies of ~10-GHz shear waves are not expected based on the viscosity, etc. This assumption is relaxed in the Appendix and the effect of evanescent shear waves on the surface-boundary conditions is analyzed. In this section it will be explicitly assumed that only longitudinal waves exist.

The local displacements of the incident and reflected sound waves associated with the μth mode are written

$$\vec{u}^{\mu}(\vec{r},t)=\tfrac{1}{2}u_0^{\mu}e^{i(\Omega t-q_{\parallel}x)}\left[\left(\hat{i}\,\frac{q_{\parallel}}{q}-\hat{k}\,\frac{q_{\perp}}{q}\right)e^{iq_{\perp}z}+\Gamma\left(\hat{i}\,\frac{q_{\parallel}}{q}+\hat{k}\,\frac{q_{\perp}}{q}\right)e^{-iq_{\perp}z}\right]+\text{c.c.} \tag{4}$$

Here u_0^{μ} is the mode amplitude, $|\Gamma|=1$ (standing-wave condition) and the wave vectors are $\vec{q}=(\hat{i}q_{\parallel}\mp\hat{k}q_{\perp})$ with $q_{\parallel}^2+q_{\perp}^2=\Omega^2/v_L^2$. As discussed in Sec. II, $T_{zz}=0$ at $z=0$, i.e.,

$$-\tfrac{1}{2}i\rho v_L^2\,\frac{q_{\perp}^2}{q}\,u_0^{\mu}e^{i(\Omega t-q_{\parallel}x)}(1+\Gamma)=0\,, \tag{5}$$

which gives $\Gamma=-1$. Therefore the normal mode is

$$\vec{u}^{\mu}(\vec{r},t)=\frac{1}{2}u_0^{\mu}e^{i(\Omega t-q_{\parallel}x)}\left[\hat{i}\left(2i\,\frac{q_{\parallel}}{q}\sin(q_{\perp}z)\right)-\hat{k}\left(\frac{2q_{\perp}}{q}\cos(q_{\perp}z)\right)\right]+\text{c.c.} \tag{6}$$

If the stress-free boundary conditions were also imposed at the yz and xz planes, then standing-wave resonances would also be obtained over the x and y coordinates, respectively.

Normal modes are thermally excited resonances of the whole medium and the resonances along the x and y axes must also be included. Therefore the energy associated with the fields described by Eq. (6) is only $\frac{1}{4}$ of the normal mode excitation energy, i.e., $\frac{1}{4}K_BT$ for $K_BT\gg\hbar\Omega$. Writing the average energy of the μth mode as twice the average kinetic energy, i.e.,

$$\langle E^{\mu}\rangle=\frac{K_BT}{4}=\rho\int_V\langle|\dot{\vec{u}}^{\mu}(\vec{r},t)|^2\rangle\,dV \tag{7}$$

yields

$$\langle|u_0^{\mu}|^2\rangle=K_BT/4\rho\Omega^2V\,, \tag{8}$$

where K_B is Boltzmann's constant and V is the volume of the sample. The allowed wave vectors for the three-dimensional resonances are described by $q_x=n_x\pi/2L_x$, $q_y=n_y\pi/2L_y$, and $q_z=n_z\pi/2L_z$ where n_x, n_y, and n_z are integers. For example, a plate surface at $z=2L_z$ must also be stress free and therefore the x component of the field must vanish at this point, i.e., $\sin(q_{\perp}2L_z)=0$. This gives $q_z=q_{\perp}=n_z\pi/2L_z$ as asserted above. In the standard acoustical terminology[24] the resonance in the z dimension is separated into symmetric (s) and antisymmetric modes (a) with allowed wave vectors $q_z=n_z(2\pi/2L_z)$ for each. Therefore the density of states in $\vec{q}$ space for both modes is $4V/(2\pi)^3$. Summations over the allowed modes μ can be replaced by an integral over $\vec{q}$ space, i.e.,

$$\sum_{\mu}\to4\,\frac{V}{(2\pi)^3}\int|d\vec{q}| \tag{9}$$

for both s and a modes. This substitution is valid for samples with dimension $L_z(\ll L_x$ and $L_y)$ such that $q_{\perp}L_z\gg1$ for all the $q_{\perp}$ of interest, i.e., the modes are closely spaced in $\vec{q}$ space. Using the relations $q_{\parallel}^2+q_{\perp}^2=\Omega^2/v_L^2$ and $dq_{\perp}=\Omega\,d\Omega/v_L(\Omega^2-\Omega_L^2)^{1/2}$, this integral can be rewritten in terms of $\vec{q}_{\parallel}$ and Ω as

$$\frac{4V}{(2\pi)^3}\int|d\vec{q}_{\parallel}|\int\frac{\Omega\,d\Omega}{v_L(\Omega^2-\Omega_L^2)^{1/2}}\,, \tag{10}$$

with $\Omega_L=q_{\parallel}v_L$. Finally we note that Ω_L is the smallest frequency possible for a mode characterized by $\vec{q}_{\parallel}$.

IV. ACOUSTIC MODES – SOLIDS

In this section the acoustical modes appropriate to a finite isotropic medium are discussed.

Consider again the geometry of Fig. 1. The shear waves polarized in the plane of the surface, i.e., along the y axis, can be decoupled from the x-z-polarized shear and longitudinal modes. Thus the normal modes (characterized by $\vec{q}_{\parallel}$ and Ω) consist of a y-polarized standing-wave shear mode and two modes which are linear combinations of longitudinal and shear waves polarized in the x-z plane. In addition there are also surface phonons on each surface which are characterized by $\vec{q}_{\parallel}$ only (i.e., $\Omega_R=q_{\parallel}v_R$, where v_R is the Rayleigh wave velocity). It proves convenient to discuss the x-z-polarized modes in three distinct regions characterized by a fixed $\vec{q}_{\parallel}$ and variable Ω. First the parameter $\Omega_T=q_{\parallel}v_T$ is defined where v_T is the shear wave velocity. Region I denotes the frequency range $\Omega>\Omega_L$, region II the range $\Omega_L>\Omega>\Omega_T$, and region III the surface phonons at $\Omega_R<\Omega_T$.

A. y-polarized modes

This case is the simplest one to analyze for a solid and is formally identical to the system analyzed in Sec. III for liquids. The standing-wave field has the form

$$\vec{u}^{\mu}(\vec{r}, t) = \tfrac{1}{2} u_0^{\mu} \hat{j} e^{i(\Omega t - q_{\parallel} x)} (e^{i q_{\perp} z} + \Gamma e^{-i q_{\perp} z}) + \text{c.c.} \qquad (11)$$

and ensuring that $T_{zy} = 0$ leads to $\Gamma = 1$. Here $q_{\parallel}^2 + q_{\perp}^2 = \Omega^2 / v_T^2$ and for a finite sample the symmetric and antisymmetric fields are degenerate in form. The pertinent wave vectors are illustrated in Fig. 2(a). It is also easy to show that normalization leads to Eq. (8) for $\langle |u_0^{\mu}|^2 \rangle$ and that the density of states in wave-vector space is $4V/(2\pi)^3$. The summation over the acoustical modes μ is replaced for this case by

$$\frac{4V}{(2\pi)^3} \int |d\vec{q}_{\parallel}| \int \frac{\Omega \, d\Omega}{v_T (\Omega^2 - \Omega_T^2)^{1/2}} \,. \qquad (12)$$

B. Region I

The analysis of modes polarized in the x-z plane is more complex than in the previous case. In the general case the field is written

$$\vec{u}^{\mu}(\vec{r}, t) = \frac{1}{2} u_0^{\mu} e^{i(\Omega t - q_{\parallel} x)} \sum_{\nu'=1}^{4} \vec{A}^{(\nu')} e^{-i q_{\perp}^{(\nu')} z} + \text{c.c.} \qquad (13)$$

for both the symmetric and antisymmetric modes. The summation over ν' is over all the x-z-polarized acoustical modes with a given $\vec{q}_{\parallel}$ and Ω which satisfy the wave equation (1).

In region I the acoustical modes consist solely of propagating shear and longitudinal waves. The terms $\nu' = 1$, 2, 3, and 4 refer, respectively, to the upward shear, downward shear, upward longitudinal and downward longitudinal traveling waves. Here

$$\begin{aligned} \vec{A}^{(1)} &= (q_{\perp}^t / q_t, 0, q_{\parallel}/q_t) \,, \\ \vec{A}^{(2)} &= e^{i\psi_\nu} (q_{\perp}^t / q_t, 0, -q_{\parallel}/q_t) \,, \\ \vec{A}^{(3)} &= \Gamma^{\nu} (q_{\parallel}/q_l, 0, -q_{\perp}^l / q_l) \,, \\ \vec{A}^{(4)} &= \Gamma^{\nu} e^{i\psi'_\nu} (q_{\parallel}/q_l, 0, q_{\perp}^l / q_l) \,, \end{aligned} \qquad (14)$$

where $\nu = 1, 2$ refers to the symmetric and antisymmetric modes. Furthermore, $q_t^2 = q_{\parallel}^2 + q_{\perp}^{t2} = \Omega^2 / v_T^2$, $q_l^2 = q_{\parallel}^2 + q_{\perp}^{l2} = \Omega^2 / v_L^2$, $q_{\perp}^{(1)} = -q_{\perp}^t$, $q_{\perp}^{(2)} = q_{\perp}^t$, $q_{\perp}^{(3)} = -q_{\perp}^l$, and $q_{\perp}^{(4)} = q_{\perp}^l$. The appropriate wave vectors for the ν' modes are shown in Fig. 2(b).

The surface boundary conditions require that $T_{zx} = T_{zz} = 0$ at $z = 0$. Evaluating the stresses

$$T_{zx} = -\frac{1}{2} i c_{44} \left(\frac{q_{\parallel}^2 - q_{\perp}^{t2}}{q_t} (1 - e^{i\psi_\nu}) - \frac{2 q_{\parallel} q_{\perp}^l}{q_l} \Gamma^{\nu} (1 - e^{i\psi'_\nu}) \right) = 0 \qquad (15)$$

and

$$T_{zz} = i c_{44} \frac{q_{\parallel} q_{\perp}^t}{q_t} (1 - e^{i\psi_\nu}) - \tfrac{1}{2} i \Gamma^{\nu} \left(q_l c_{11} - 2 c_{44} \frac{q_{\parallel}^2}{q_l} \right) (1 + e^{i\psi'_\nu}) = 0 \,. \qquad (16)$$

By inspection, $T_{zx} = 0$ for $\psi_1 = \psi'_1 = 0$ and a symmetric mode is formed for

$$\Gamma^{(1)} = \frac{2\Omega_T^2 (\Omega^2 - \Omega_T^2)^{1/2}}{\Omega_L (\Omega^2 - 2\Omega_T^2)} \,, \qquad (17)$$

a condition which yields $T_{zz} = 0$. Noting that $T_{zz} = 0$ for $\psi_2 = \psi'_2 = \pi$, the antisymmetric mode is formed by requiring that $T_{zx} = 0$ which yields

$$\Gamma^{(2)} = \frac{2\Omega_T^2 - \Omega^2}{2\Omega_T (\Omega^2 - \Omega_L^2)^{1/2}} \,. \qquad (18)$$

This is the only case for which the symmetric and antisymmetric solutions are not identical in form.

Each of these modes is normalized to an average energy of $\frac{1}{4} K_B T$ as discussed in Sec. III. Proceeding as in the liquid case,

$$\langle |u_0^{\mu}|^2 \rangle = \frac{K_B T}{2 V \rho \Omega^2 \sum_{\nu'} |\vec{A}^{\nu'}|^2} \,. \qquad (19)$$

It can be shown that

$$\sum_{\nu'} |\vec{A}^{\nu'}|^2 = \frac{2\Omega_L^2 (\Omega^2 - 2\Omega_T^2)^2 + 8\Omega_T^4 (\Omega^2 - \Omega_T^2)}{\Omega_L^2 (\Omega^2 - 2\Omega_T^2)^2} \qquad (20)$$

$$= \frac{4\Omega_T^2 (\Omega^2 - \Omega_L^2) + (2\Omega_T^2 - \Omega^2)^2}{2\Omega_T^2 (\Omega^2 - \Omega_L^2)} \qquad (21)$$

for the symmetric and antisymmetric cases, re-

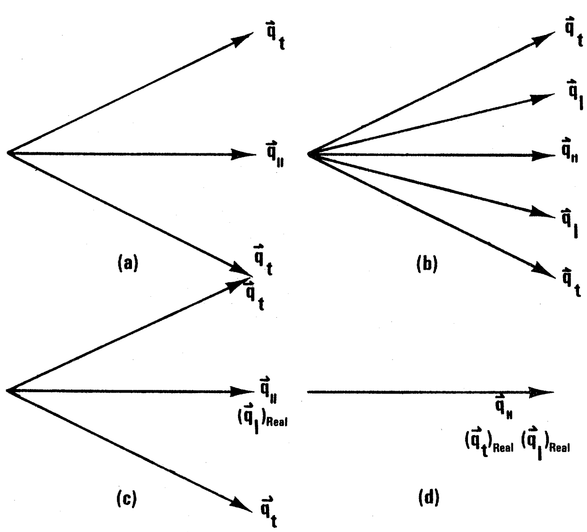

FIG. 2. Real part of the acoustical wave vectors associated with (a) the y-polarized shear mode; the x-z-polarized modes in the frequency range (b) $\Omega > \Omega_L$, (c) $\Omega_L > \Omega > \Omega_T$, and (d) $\Omega = \Omega_R$.

spectively.

Despite the complex nature of these fields, summations over the acoustical modes designated μ can be replaced by an integral over wave-vector space. Stratton[26] has shown that the density of states is $4V/(2\pi)^3$ for a wavevector $\vec{q}$ with $q_\perp = q_\perp^t + q_\perp^l = (2\pi/2L_z)n_z$. This relation is correct for an average over a number of neighboring states. Noting that $dq_\perp = dq_\perp^t + dq_\perp^l$, then

$$dq_\perp = \frac{v_L(\Omega^2-\Omega_L^2)^{1/2} + v_T(\Omega^2-\Omega_T^2)^{1/2}}{v_T(\Omega^2-\Omega_T^2)^{1/2} v_L(\Omega^2-\Omega_L^2)^{1/2}}\,\Omega\, d\Omega \qquad (22)$$

and

$$\sum_\mu \rightarrow \frac{4V}{(2\pi)^3}\int |d\vec{q}_\parallel| \int \frac{v_L(\Omega^2-\Omega_L^2)^{1/2} + v_T(\Omega^2-\Omega_T^2)^{1/2}}{v_L(\Omega^2-\Omega_L^2)^{1/2} v_T(\Omega^2-\Omega_T^2)^{1/2}}\,\Omega\, d\Omega . \qquad (23)$$

C. Region II

In this region only the shear waves are propagating modes whereas the longitudinal fields become evanescent at both the top and bottom surfaces of the plate. The field amplitudes for $\nu' = 1$ and 2 in Eq. (13) are identical to those defined by Eq. (14). The remaining terms decay exponentially into the medium at the upper ($\nu' = 3$) and lower surface ($\nu' = 4$), with

$$\vec{A}^{(3)} = \frac{\Gamma^\nu}{(1+\gamma^2)^{1/2}}(1, 0, i\gamma),$$
$$\vec{A}^{(4)} = \frac{\Gamma^\nu}{(1+\gamma^2)^{1/2}} e^{-2L_z\gamma q_\parallel}(1, 0, -i\gamma), \qquad (24)$$

with $\gamma^2 = 1 - \Omega^2/\Omega_L^2$, $q_\perp^{(3)} = -i\gamma q_\parallel$, and $q_\perp^{(4)} = i\gamma q_\parallel$. For thick samples, i.e., $1 \gg \exp(-2L_z\gamma q_\parallel)$, the symmetric and antisymmetric solutions are degenerate in form and requiring that $T_{xz} = T_{zz} = 0$ yields

$$\Gamma = \frac{4(\Omega^2-\Omega_T^2)^{1/2}(2\Omega_T^2-\Omega^2)\Omega_T^2(1+\gamma^2)^{1/2}}{\Omega[-(2\Omega_T^2-\Omega^2)^2 + 4i\gamma\Omega_T^3(\Omega^2-\Omega_T^2)^{1/2}]} \qquad (25)$$

and

$$\cot\left(\frac{\psi}{2}\right) = \frac{(2\Omega_T^2-\Omega^2)^2}{4\gamma\Omega_T^3(\Omega^2-\Omega_T^2)^{1/2}} . \qquad (26)$$

The real parts of the acoustical wave vectors are shown in Fig. 2(c). (The wave vectors associated with the evanescent modes have imaginary components.)

The mode energy is normalized in the usual way and the normalization is given by Eq. (19). For thick samples the energy associated with the evanescent waves can be neglected compared to the energy carried by the shear modes and $\sum_{\nu'}|\vec{A}^{\nu'}|^2 = 2$. Therefore

$$\langle |u_0^\mu|^2 \rangle = K_B T/4\rho\Omega^2 V . \qquad (27)$$

This approximation is valid everywhere except for a small frequency region $\Delta\Omega \sim \Omega_L/8L_z^2 q_\parallel^2$ just below the longitudinal mode cut-off frequency Ω_L.

The density of states is governed principally by the standing-wave shear part of the mode, except for the small frequency region $\Delta\Omega$. It is given by $4V/(2\pi)^3$ and the summation over the phonon states is given by

$$\frac{4V}{(2\pi)^3}\int |d\vec{q}_\parallel| \int \frac{\Omega\, d\Omega}{(\Omega^2-\Omega_T^2)^{1/2} v_T} . \qquad (28)$$

D. Region III

For frequencies below the shear cut-off frequency only one phonon mode, a surface wave,[27] exists for each value of $\vec{q}_\parallel$. All of the acoustical field solutions are evanescent and the energy is confined to the upper and lower surfaces. At the upper surface

$$\vec{A}^{(1)} = (-(\alpha^{(1)}\alpha^{(2)})^{1/2}, 0, i(\alpha^{(2)}/\alpha^{(1)})^{1/2})$$

and (29)

$$\vec{A}^{(2)} = (1, 0, -i\alpha^{(2)}),$$

with

$$\alpha^{(1)} = (1 - \Omega_R^2/\Omega_T^2)^{1/2},$$
$$\alpha^{(2)} = (1 - \Omega_R^2/\Omega_L^2)^{1/2}, \qquad (30)$$

and

$$q_\perp^{(1)} = -i\alpha^{(1)} \text{ and } q_\perp^{(2)} = -i\alpha^{(2)}.$$

The equivalent terms on the lower surface are

$$\vec{A}^{(3)} = e^{-2L_z\alpha^{(1)}q_\parallel}(-(\alpha^{(1)}\alpha^{(2)})^{1/2}, 0, -i(\alpha^{(2)}/\alpha^{(1)})^{1/2}),$$
$$\vec{A}^{(4)} = e^{-2L_z\alpha^{(2)}q_\parallel}(1, 0, i\alpha^{(2)}), \qquad (31)$$

and

$$q_\perp^{(3)} = i\alpha^{(1)} \text{ and } q_\perp^{(4)} = i\alpha^{(2)} .$$

The ratio Ω_R/q is evaluated from the stress-free boundary conditions which produces the Viktorov equation[27]

$$[2-(v_R/v_T)^2]^2 = 4[1-(v_R/v_L)^2]^{1/2}[1-(v_R/v_T)^2]^{1/2} . \qquad (32)$$

For a finite sample the symmetric and antisymmetric solutions are degenerate.

Here we have an energy normalization which is different to that of the bulk wave case. Since the surface waves are excitations of a two-dimensional surface, the appropriate resonances associated with the normal mode are those over the surface coordinates only. Again, $\frac{1}{4}$ of the thermal energy is involved and evaluating Eq. (7) gives

$$\langle |u_0^\mu|^2\rangle = K_B T \Big/ 4\rho\Omega_R v_R A \sum_{\nu'=1}^{2} \sum_{\eta'=1}^{2} \frac{A_j^{\nu'} A_i^{*\eta'}}{\alpha^{\nu'} + \alpha^{*\nu'}} \tag{33}$$

for both the symmetric and antisymmetric modes. No additional simplification of the denominator term will be useful and the term is left in this particular form. Furthermore, these surface excitations are characterized by $\vec{q}_\parallel$ and therefore the mode density in $\vec{q}_\parallel$ space is given by $4A/(2\pi)^2$. Any summation over the modes labeled by μ is therefore replaced by

$$\frac{4A}{(2\pi)^2} \int |d\vec{q}_\parallel| . \tag{34}$$

E. Anisotropic media

The generalization to the acoustical modes of an acoustically anisotropic medium is simple in principle but tedious in practice. The three solutions of the acoustical-wave equation are no longer pure longitudinal ($\vec{\nabla}\times\vec{u}=0$) and shear ($\vec{\nabla}\cdot\vec{u}=0$) modes. As a result, the stress-free boundary condition couples all three waves and the modes are linear combinations of standing waves composed of the two quasishear and one quasilongitudinal waves. Numerical techniques are necessary to find the relative amplitude and phase factors which lead to $T_{zj}=0$. Three such orthogonal linear combinations are possible.

V. LIGHT SCATTERING - GENERAL

There are basically two scattering mechanisms near the surface of a material, the corrugation and elasto-optical effects.

The presence of an acoustical wave at a boundary creates a surface ripple which alters the usual electromagnetic boundary conditions. This corrugation has the form $u_z = u_0^\mu \,\delta \cos(\Omega t - q_\parallel x)$ and can be considered as a travelling, sinuosoidal diffraction grating which scatters Doppler-shifted light into the "first diffraction order." This phenomenon was first used by Bergmann and Schaeffer[19] to study light scattering from generated bulk and surface waves on opaque media. Recently it has been used as a diagnostic tool for surface acoustical wave devices,[20] as the readout mechanism for acoustical microscopes[21] and to investigate shear waves at semiconductor surfaces.[22]

This acousto-optical interaction has been analyzed previously in a number of ways. Diffraction[28] and Helmholtz[29] integrals were used to describe the diffraction of light by low-frequency-generated surface acoustical waves. However these techniques are valid for $q_\parallel/k \ll 1$, where k is the optical wave vector. Another approach[23] is to examine the continuity of the usual electromagnetic boundary conditions across the corrugated interface. It can be shown that either the tangential electric or magnetic field, or both are discontinuous across the moving surface. The additional radiation fields required to satisfy the boundary conditions correspond to the Brillouin-scattered fields. It is this latter approach which will be pursued in this paper.

The second mechanism to be analyzed is the elasto-optical effect which is the well-known source of Brillouin scattering in "infinite" media. Included in this category are all phenomena which scatter light from sound waves in the bulk of a material. (The special case of conductivity fluctuations in a metal will be discussed separately.) The general elasto-optical interaction is described by

$$P_i = -\frac{1}{\epsilon_0}\,\epsilon_{im}\epsilon_{jn}\,p_{mnkl}\;\frac{1}{2}\left(\frac{\partial u_k}{\partial x_l} + \frac{\partial u_l}{\partial x_k}\right)E_j , \tag{35}$$

where p_{mnkl} is the elasto-optical tensor and $\vec{P}$ is the polarization field created by the interaction between the acoustical strain and the incident optical field E_j. These polarization fields radiate electromagnetic waves which are then observed as the scattered light. In mathematical terms the polarizations are sources for an electromagnetic-wave equation and total fields are found which satisfy both the driven-wave equation and the electromagnetic boundary conditions.

It proves convenient to analyze directly the source of the elasto-optical interaction for a metal, namely, the conductivity effect identified by Dil and Brody.[8] Density fluctuations associated with a sound wave produce fluctuations in the density of a "free-electron gas" in a good metal. Since the local conductivity is proportional to the local electron density, an incident optical field produces oscillating currents which in turn radiate scattered fields. In the mathematical analysis the currents drive an electromagnetic-wave equation and total fields are derived which also satisfy the boundary conditions.

VI. LIGHT SCATTERING - CORRUGATION EFFECT

A general theory of light scattering by surface corrugations on a dielectric transparent material has recently been reported[23] by one of us and essentially the same formalism will be extended

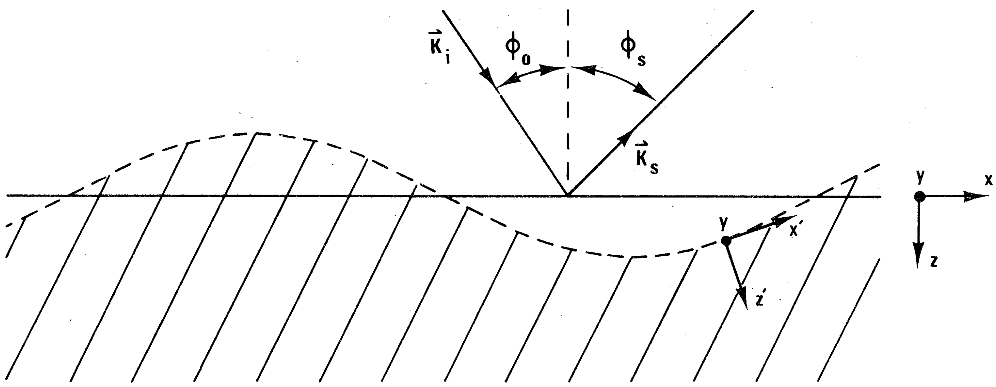

FIG. 3. Light-scattering geometry.

to opaque media. All experiments on surfaces reported to date[7,9] have dealt with geometries in which the incident and scattered wave vectors were coplanar with the normal to the surface. Only this geometry as illustrated in Fig. 3 is considered here. (The more general case was analyzed for dielectric media in Ref. 23.) Both s- and p-polarized light, i.e., with the optical electric field parallel to the surface or in the plane defined by the surface normal and the optical wave vector respectively, will be treated.

The analysis is based on matching electromagnetic boundary conditions across a moving surface. Therefore fields must be evaluated in a coordinate system fixed to the oscillating surface, i.e., the x', y, z' axes shown in Fig. 3. The transformations relating a vector $\vec{R} \equiv (R_x, R_y, R_z)$ specified originally in the stationary x, y, z coordinate system to the same vector $\vec{R} \equiv (R_x', R_y', R_z')$ in the x', y, z' system is given by

$$R_x' = R_x + R_z \sin\xi \,, \quad R_z' = R_z - R_x \sin\xi \tag{36}$$

for small rotation angles ξ. For a surface corrugation of the form $u_z = u_0^{\parallel}\delta\cos(\Omega t - q_{\parallel}x)$,

$$\frac{\partial u_z}{\partial x} = \tan\xi \simeq u_0^{\parallel}\delta q_{\parallel}\sin(\Omega t - q_{\parallel}x)\,.$$

Note that these transformations indicate that the normal field components contribute to the tangential fields across the rippled interface.

A. p-polarized incidence

Consider first the electromagnetic fields and boundary conditions in the absence of sound waves at the surface of an opaque material of refractive index n_m. The incident, reflected and transmitted fields are of the form

$$\vec{E}_i = \tfrac{1}{2}E_0(\hat{i}\cos\phi_0 - \hat{k}\sin\phi_0) \times \exp[i(\omega_0 t - k_{\parallel}x - k\cos\phi_0 z)] + \text{c.c.}\,, \tag{37}$$

$$\vec{E}_r = \tfrac{1}{2}E_0'(\hat{i}\cos\phi_0 + \hat{k}\sin\phi_0) \times \exp[i(\omega_0 t - k_{\parallel}x + k\cos\phi_0 z)] + \text{c.c.}\,, \tag{38}$$

$$\vec{E}_t = \tfrac{1}{2}E_0''(-\hat{i}in_m\beta - \hat{k}\sin\phi_0) \times \exp[i(\omega_0 t - k_{\parallel}x) - \beta n_m kz] + \text{c.c.}\,, \tag{39}$$

respectively, for light of wave vector $\vec{k}$ and frequency ω_0 incident at an angle ϕ_0 relative to the surface normal, see Fig. 3. Here $k_{\parallel} = k\sin\phi_0$ and $\beta^2 = \sin^2\phi_0/n_m^2 - 1$. For example, for a good metal $|n_m^2| \gg 1$ and $\beta = -i$. The continuity of E_x and H_y at $z=0$ yields the usual Fresnel relations

$$E_0'/E_0 = (\beta - in_m\cos\phi_0)/(\beta + in_m\cos\phi_0) \tag{40}$$

and

$$E_0''/E_0 = 2i\cos\phi_0/(n_m\beta + in_m^2\cos\phi_0)\,. \tag{41}$$

We now assume the presence of sound waves at the interface. As a result the electromagnetic boundary conditions must now be satisfied across the moving surface [i.e., at $z = u_0^{\parallel}\delta\cos(\Omega t - q_{\parallel}x)$] in the x', y, z' coordinate system. Expanding terms of the type

$$\exp[ik\cos\phi_0\delta\cos(\Omega t - q_{\parallel}x)]$$

as Bessel functions, applying the transformation in Eq. (36) and assuming $1 \gg u_0^{\parallel}\delta q_{\parallel}$ and $1 \gg u_0^{\parallel}\delta k$, then the tangential fields[23] at $z \simeq 0$ are

(i) *incident*

$$E_x = \frac{1}{2}u_0^{\parallel}\delta E_0 i\left(-\frac{k\cos^2\phi_0}{2} \pm \frac{q_{\parallel}\sin\phi_0}{2}\right)\exp\{i[(\omega_0 \pm \Omega)t - (k_{\parallel} \pm q_{\parallel})x]\} + \text{c.c.}\,, \tag{42}$$

$$H_y = \frac{1}{2} u_0^\mu \delta E_0 i \left(-\frac{k^2 \cos\phi_0}{2\omega_0\mu_0}\right) \exp\{i[(\omega_0 \pm \Omega)t - (k_\parallel \pm q_\parallel)x]\} + \text{c.c.}\,; \tag{43}$$

(ii) *reflected*

$$E_x = \frac{1}{2} u_0^\mu \delta E_0' i \left(\frac{k\cos^2\phi_0}{2} \mp \frac{q_\parallel \sin\phi_0}{2}\right) \exp\{i[(\omega_0 \pm \Omega)t - (k \pm q_\parallel)x]\} + \text{c.c.}\,, \tag{44}$$

$$H_y = \frac{1}{2} u_0^\mu \delta E_0' i \left(-\frac{k^2 \cos\phi_0}{2\omega_0\mu_0}\right) \exp\{i[(\omega_0 \pm \Omega)t - (k_\parallel \pm q_\parallel)x]\} + \text{c.c.}\,, \tag{45}$$

(iii) *transmitted*

$$E_x = \frac{1}{2} u_0^\mu \delta E_0'' i \left(\frac{k\beta^2}{2} \pm \frac{q_\parallel \sin\phi_0}{2}\right) \exp\{i[(\omega_0 \pm \Omega)t - (k_\parallel \pm q_\parallel)x]\} + \text{c.c.}\,, \tag{46}$$

$$H_y = \frac{1}{2} u_0^\mu \delta E_0'' i \left(-\frac{k^2\beta n_m^2}{2\omega_0\mu_0}\right) \exp\{i[(\omega_0 \pm \Omega)t - (k_\parallel \pm q_\parallel)x]\} + \text{c.c.} \tag{47}$$

It can now easily be shown that E_x and H_y are no longer continuous at $z=0$. For example, $\Delta E_x = (E_x)_{\text{incid}} + (E_x)_{\text{reflec}} - (E_x)_{\text{trans}} \neq 0$. Evaluating relative to the air side of the interface gives

$$\Delta E_x = -\frac{1}{2}\, \frac{\sin\phi_0 \cos\phi_0 (n_m^2 - 1)}{n_m\beta + i n_m^2 \cos\phi_0}\, u_0^\mu \delta E_0 (k_\parallel \pm q_\parallel) \exp\{i[(\omega_0 \pm \Omega)t - (k_\parallel \pm q_\parallel)x]\} + \text{c.c.} \tag{48}$$

and

$$\Delta H_y = \frac{1}{2}\, \frac{i \cos\phi_0 (n_m^2 - 1)\beta k^2}{\omega_0\mu_0(\beta + i n_m \cos\phi_0)}\, u_0^\mu \delta E_0 \exp\{i[(\omega_0 \pm \Omega)t - (k_\parallel \pm q_\parallel)x]\} + \text{c.c.} \tag{49}$$

Thus the corrugation effect is manifested in terms of discontinuities in the usual electromagnetic boundary conditions.

Continuity of the tangential electromagnetic boundary conditions is satisfied by the total fields. The additional fields are solutions to the homogeneous wave equation in air, i.e.,

$$\vec{\mathbf{E}}_a = \frac{1}{2} A_c u_0^\mu \left(\hat{i}\,\frac{k_z}{k} + \hat{k}\,\frac{k_\parallel \pm q_\parallel}{k}\right) \exp\{i[(\omega_0 \pm \Omega)t - (k_\parallel \pm q_\parallel)x + k_z z]\} + \text{c.c.}\,, \tag{50}$$

and in the metal, i.e.,

$$\vec{\mathbf{E}}_m = \frac{1}{2} B_c u_0^\mu \left[-\hat{i} i\beta' n_m - \hat{k}\left(\frac{k_\parallel \pm q_\parallel}{k}\right)\right] \exp\{i[(\omega_0 \pm \Omega)t - (k_\parallel \pm q_\parallel)x] - \beta' n_m k z\} + \text{c.c.}\,, \tag{51}$$

respectively, with $k_z^2 = k^2 - (k_\parallel \pm q_\parallel)^2$ and $\beta'^2 = (k_\parallel \pm q_\parallel)^2/n_m^2 k^2 - 1$. The field designated by $\vec{\mathbf{E}}_a$ propagates away from the surface and forms part of the total field observed in the experiment. The scattering angle ϕ_s (shown in Fig. 3) is given by $\cos\phi_s = k_z/k$. Evaluating gives

$$A_c = \frac{ik\cos\phi_0(n_m^2 - 1)[k\beta\beta' + \sin\phi_0(k_\parallel \pm q_\parallel)]}{(i n_m k_z + \beta' k)(\beta + i n_m \cos\phi_0)}\, \delta E_0\,. \tag{52}$$

The term

$$H_p = \frac{ik\cos\phi_0(n_m^2 - 1)[k\beta\beta' + \sin\phi_0(k_\parallel \pm q_\parallel)]}{(i n_m k_z + \beta' k)(\beta + i n_m \cos\phi_0)} \tag{53}$$

is basically a geometrical factor so that we now write $A_c = H_p \delta E_0$. Finally we note that the scattered fields have the same polarization as the incident field, i.e., no depolarized scattering occurs via the corrugation mechanism.

Only partial wave vector conservation occurs in this acousto-optical interaction. The components of the incident and scattered optical wave vectors uniquely determine the value of $q_\parallel$. This implies that wave-vector conservation is valid only in the plane of the surface, a feature common to other scattering phenomena at surfaces.[30] Furthermore, the light scattering originates from a phonon continuum characterized by a fixed value of $\vec{q}_\parallel$ and therefore the frequency shift of the scattered light starts at some cutoff frequency $\Omega = q_\parallel v$ and extends in principle to very high frequencies.

B. s-polarized incidence

The analysis for this case is exactly the same as for the previous p-polarized geometry. For an incident field of the form

$$\vec{E}_i = \tfrac{1}{2}\hat{j} E_0 \exp[i(\omega_0 t - k_{\parallel} x - k\cos\phi_0 z)] + \text{c.c.}, \tag{54}$$

it can easily be shown that $\Delta E_y = 0$ and

$$\Delta H_x = \frac{-ik^2 \cos\phi_0 (n_m^2 - 1) u_0^\mu \delta E_0}{2\omega_0 \mu_0 (\cos\phi_0 - i n_m \beta)} \times \exp\{i[(\omega_0 \pm \Omega)t - (k_{\parallel} \pm q_{\parallel})x]\} + \text{c.c.} \tag{55}$$

Again additional solutions to the homogeneous wave equation are required in the air and metal in order to satisfy boundary conditions. The scattered field has the form

$$\vec{E}_a = \tfrac{1}{2}\hat{j} u_0^\mu A_c \exp\{i[(\omega_0 \pm \Omega)t - (k_{\parallel} \pm q_{\parallel})x + k_z z]\} + \text{c.c.} \tag{56}$$

with

$$A_c = H_s \delta E_0 \tag{57}$$

and

$$H_s = \frac{-ik^2 \cos\phi_0 (n_m^2 - 1)}{(\cos\phi_0 - i n_m \beta)(i\beta' n_m k - k_z)} . \tag{58}$$

Therefore the scattered fields are again of the same polarization as the incident field.

C. Specific cases

It has been shown in the preceding discussion that the scattered fields are directly proportional to the corrugation δ. This term is now evaluated for the acoustical modes of Secs. II–IV.

Liquid:

$$\delta = -2(\Omega^2 - \Omega_L^2)^{1/2}/\Omega . \tag{59}$$

Solid y-polarized shear:

$$\delta = 0 . \tag{60}$$

Solid x-z polarized waves:

region I,

$$\delta = 0 \quad \text{(symmetric mode)}, \tag{61}$$

$$\delta = \Omega/\Omega_T \quad \text{(antisymmetric mode)}; \tag{62}$$

region II,

$$\delta = \frac{-4i\gamma\Omega\Omega_T^2 (\Omega^2 - \Omega_T^2)^{1/2}}{(2\Omega_T^2 - \Omega^2)^2 - 4i\gamma\Omega_T^3 (\Omega^2 - \Omega_T^2)^{1/2}} ; \tag{63}$$

region III,

$$\delta = -i\alpha^{(2)}[1 - 1/(\alpha^{(1)}\alpha^{(2)})^{1/2}] . \tag{64}$$

These results indicate that only the x-z-polarized modes contribute to this scattering mechanism. Note that the shear wave components of the x-z-polarized modes contribute to the polarized scattering, a situation which does not occur for Brillouin scattering in "infinite" media. The preceding formulas are for the upshift case $(\omega_0 + \Omega)$ and conversion to $(\omega_0 - \Omega)$ requires taking the complex conjugates of Eqs. (59)–(64).

VII. LIGHT SCATTERING–CONDUCTIVITY FLUCTUATIONS

The acousto-optical mechanism appropriate to a metal which can be described by a "free-electron gas" is discussed in this section. In such a medium the bound electrons associated with the ions are effectively screened by the electron gas and the effects of dipole radiation from the bound electrons becomes negligible. However propagating density waves (longitudinally polarized excitations) produce local fluctuations in the density of the free-electron gas and therefore in the local conductivity, i.e., $\Delta\sigma/\sigma = \Delta\rho/\rho$. For sound waves described by Eq. (13), the density fluctuations $(\Delta\rho/\rho = \vec{\nabla}\cdot\vec{u})$ are given by

$$\Delta\rho/\rho = \frac{1}{2} u_0^\mu e^{i(\Omega t - q_{\parallel} x)} \sum_{\nu'} \Delta\rho^{\nu'} e^{i q_{\perp}^{\nu'} z} + \text{c.c.}, \tag{65}$$

with

$$\Delta\rho^{\nu'} = -i q_{\parallel} A_x^{\nu'} + i q_{\perp}^{\nu'} A_z^{\nu'} . \tag{66}$$

Therefore the conductivity fluctuation produced by the μth acoustical mode is

$$\Delta\sigma^\mu = \tfrac{1}{2}\sigma u_0^\mu e^{i(\Omega t - q_{\parallel} x)} \sum_{\nu'} \Delta\rho^{\nu'} e^{i q_{\perp}^{\nu'} z} + \text{c.c.} \tag{67}$$

A. p-polarized incidence

The appropriate incident, reflected and transmitted fields are given by Eqs. (37)–(41) for the p-polarized geometry. Fluctuating currents $(\vec{J} = \Delta\sigma\vec{E}_t)$ of the form

$$\vec{J} = \frac{1}{4}\sigma u_0^\mu E_0''(-\hat{i} i n_m \beta - \hat{k}\sin\phi_0)\Big[\exp[i(\omega_0 + \Omega)t - i(k_{\parallel} + q_{\parallel})x] \sum_{\nu'} \Delta\rho^{\nu'} e^{-(n_m \beta k - i q_{\perp}^{\nu'})z} + \exp[i(\omega_0 - \Omega)t - i(k_{\parallel} - q_{\parallel})x] \sum_{\nu'} \Delta\rho^{*\nu'} e^{-(n_m \beta k + i q_{\perp}^{*\nu'})z}\Big] + \text{c.c.} \tag{68}$$

are created by the sound waves and radiate electromagnetic waves at the frequencies $\omega_0 \pm \Omega$. Only the downshift case will be treated further for the sake of brevity. These currents act as sources for the wave equation for the vector potential $\vec{A}$ and for the scalar potential ϕ via the Lorentz condition or the conservation of charge condition.[31] Therefore

$$\vec{\nabla}^2 \vec{A} - (n_m^2/c^2)\ddot{\vec{A}} = -\mu_0 \vec{J} \quad \text{and} \quad \vec{\nabla}\cdot\vec{A} + (n_m^2/c^2)\dot{\phi} = 0 \tag{69}$$

are satisfied and the usual electromagnetic fields recovered from $\vec{E} = -\vec{\nabla}\phi - \dot{\vec{A}}$ and $\vec{B} = \vec{\nabla}\times\vec{A}$. The resulting tangential fields

$$H_y = \tfrac{1}{4} i\sigma u_0^\mu E_0'' \exp[i(\omega_0 - \Omega)t - i(k_\parallel - q_\parallel)x] \sum_{\nu'} \frac{\Delta\rho^{*\nu'}[\sin\phi_0(k_\parallel - q_\parallel) - n_m\beta(n_m\beta k + iq_\perp^{*\nu'})]e^{-(\beta n_m k + iq_\perp^{*\nu'})z}}{(\beta n_m k + iq_\perp^{*\nu'})^2 - (\beta' n_m k)^2} + \text{c.c.} \tag{70}$$

and

$$E_x = \tfrac{1}{4}\sigma \frac{u_0^\mu c E_0'' \exp[i(\omega_0 - \Omega)t - i(k_\parallel - q_\parallel)x]}{k n_m^2} \sum_{\nu'} \frac{\Delta\rho^{*\nu'}[k^2\beta'^2 n_m^3 - \sin\phi_0(k_\parallel - q_\parallel)(\beta n_m k + iq_\perp^{*\nu'})]e^{-(\beta n_m k + iq_\perp^{*\nu'})z}}{(\beta n_m k + iq_\perp^{*\nu'})^2 - (\beta' n_m k)^2} + \text{c.c.} \tag{71}$$

exist only in the acousto-optical interaction region and do not propagate away from the surface. When evaluated at the surface, both fields give rise to discontinuities in the boundary conditions and additional fields of the form of Eqs. (50) and (51) with amplitudes A_e and B_e are required. Writing $\sigma = -i\omega_0\epsilon(n_m^2 - 1)$ for good metals and ensuring that the usual boundary conditions are satisfied yields

$$A_e = H_p' E_0 \sum_{\nu'} \frac{\Delta\rho^{*\nu'}}{(\beta + \beta')n_m k + iq_\perp^{*\nu'}} , \tag{72}$$

with

$$H_p' = \frac{ik\cos\phi_0(n_m^2 - 1)[k\beta\beta' + (k_\parallel - q_\parallel)\sin\phi_0/n_m^2]}{(in_m k_z + \beta' k)(\beta + in_m\cos\phi_0)} . \tag{73}$$

The scattered fields are similar to those obtained for the corrugation case, i.e., the scattered fields are not depolarized and a continuum of phonons characterized by a single value of $\vec{q}_\parallel$ contributes to the scattered fields. Note that the geometric factor is not quite the same for the corrugation (H_p) and conductivity (H_p') mechanisms.

B. s-polarized incidence

The analysis for this geometry is exactly the same as for the previous case. Vector and scalar potentials ($\phi = 0$) are evaluated for the currents produced by the local density fluctuations. After some algebra it can easily be shown that the driven fields give rise to the discontinuities

$$\Delta E_y = -\tfrac{1}{4} i\sigma u_0^\mu E_0'' \mu_0 \omega_0 \exp[i(\omega_0 - \Omega)t - i(k_\parallel - q_\parallel)x] \sum_{\nu'} \frac{\Delta\rho^{*\nu'} e^{-(\beta n_m k + iq_\perp^{*\nu'})z}}{(\beta n_m k + iq_\perp^{*\nu'})^2 - (\beta' n_m k)^2} + \text{c.c.} \tag{74}$$

and

$$\Delta H_x = \tfrac{1}{4}\sigma u_0^\mu E_0'' \exp[i(\omega_0 - \Omega)t - i(k_\parallel - q_\parallel)x] \sum_{\nu'} \frac{\Delta\rho^{*\nu'}(\beta n_m k + iq_\perp^{*\nu'})e^{-(\beta n_m k + iq_\perp^{*\nu'})z}}{(\beta n_m k + iq_\perp^{*\nu'})^2 - (\beta' n_m k)^2} + \text{c.c.} \tag{75}$$

in the surface tangential fields (relative to the air side of the interface) with $E_0''/E_0 = 2\cos\phi_0/(\cos\phi_0 - in_m\beta)$. Again additional fields are required and the field scattered into the air has the form given by Eq. (56) with amplitude

$$A_e = H_s E_0 \sum_{\nu} \frac{\Delta\rho^{*\nu'}}{(\beta + \beta')n_m k + iq_\perp^{*\nu'}} . \tag{76}$$

Again only polarized scattering occurs.

C. Specific cases

It has been shown in the preceding analysis that the scattered field is proportional to

$$\sum_{\nu'} \Delta\rho^{*\nu'} / [(\beta + \beta')n_m k + iq_\perp^{*\nu'}] .$$

This term is now evaluated for the acoustical modes of Secs. II–IV for the downshift case $\omega_0 - \Omega$.

Liquid:

$$\frac{2(\Omega^2-\Omega_L^2)^{1/2}\Omega}{[n_m k(\beta+\beta')v_L]^2+\Omega^2-\Omega_L^2}. \quad (77)$$

Solid y-polarized shear:

$$0. \quad (78)$$

Solid x-z-polarized modes: *region* I,

$$\frac{4\Omega v_L\Omega_T{}^2(\Omega^2-\Omega_T^2)^{1/2}(\beta+\beta')n_m k}{\Omega_L(\Omega^2-2\Omega_T^2)\{[n_m k(\beta+\beta')v_L]^2+\Omega^2-\Omega_L^2\}} \quad \text{(symmetric)}, \quad (79)$$

$$\frac{\Omega}{\Omega_T}\frac{(2\Omega_T^2-\Omega^2)}{[n_m k(\beta+\beta')v_L]^2+\Omega^2-\Omega_L^2} \quad \text{(antisymmetric)}; \quad (80)$$

region II,

$$\frac{-4i\Omega\Omega_T^2(\Omega^2-\Omega_T^2)^{1/2}}{(2\Omega_T^2-\Omega^2)^2+4i\gamma\Omega_T^3(\Omega^2-\Omega_T^2)^{1/2}} \times\frac{(2\Omega_T^2-\Omega^2)}{\Omega_L[n_m k(\beta+\beta')v_L+(\Omega_L^2-\Omega^2)^{1/2}]}; \quad (81)$$

region III,

$$\frac{i\Omega_R^3/\Omega_L^2}{n_m k(\beta+\beta')v_R+\Omega_R(1-\Omega_R^2/\Omega_L^2)^{1/2}}. \quad (82)$$

Conversion to the upshift fields is achieved by taking the complex conjugate of Eqs. (77)–(82).

VIII. LIGHT SCATTERING–ELASTOOPTIC EFFECT

The elasto-optical mechanism is analyzed for an arbitrary opaque medium in this section. Equation (35) simplifies for an optically isotropic medium to

$$P_i=-\epsilon_0 n_m^4 p_{ijkl}\left(\frac{\partial u_x}{\partial x_l}+\frac{\partial u_l}{\partial x_k}\right)E_j. \quad (83)$$

This polarization field is the source for the driven wave equation[31]

$$\nabla^2\vec{\pi}-\frac{n_m^2}{c^2}\ddot{\vec{\pi}}=-\vec{P}/\epsilon_0 n_m^2 \quad (84)$$

for the Hertz vector $\vec{\pi}$. Total field solutions are found which satisfy Eq. (84) as well as the electromagnetic boundary conditions.

A. *p*-polarized incidence

The analysis for this geometry is essentially the same as for the conductivity case. The polarization fields for the downshift case $(\omega_0-\Omega)$ are

$$\vec{P}=-\tfrac{1}{2}\epsilon_0 n_m^2 E_0'' u_0^\mu \sum_{\nu'}\vec{P}^{\nu'}\exp[i(\omega_0-\Omega)t-i(k_\parallel-q_\parallel)x-(\beta n_m k+iq_\perp^{*\nu'})z]+\text{c.c.}, \quad (85)$$

with

$$P_x^{\nu'}=\tfrac{1}{2}n_m^2[-i\beta n_m(p_{11}A_x^{*\nu'}l_x^{*\nu'}+p_{12}A_z^{*\nu'}l_z^{*\nu'})-\sin\phi_0 p_{44}(A_x^{*\nu'}l_z^{*\nu'}+A_z^{*\nu'}l_x^{*\nu'})], \quad (86)$$

$$P_y^{\nu'}=\tfrac{1}{2}n_m^2 p_{44}(-i\beta n_m A_y^{*\nu'}l_x^{*\nu'}-\sin\phi_0 A_y^{*\nu'}l_z^{*\nu'}), \quad (87)$$

and

$$P_z^{\nu'}=\tfrac{1}{2}n_m^2[-i\beta n_m p_{44}(A_z^{*\nu'}l_x^{*\nu'}+A_x^{*\nu'}l_z^{*\nu'})-\sin\phi_0(p_{11}A_z^{*\nu'}l_z^{*\nu'}+p_{12}A_x^{*\nu'}l_x^{*\nu'})]. \quad (88)$$

Here $l_x^{\nu'}=-iq_\parallel$, $l_y^{\nu'}=0$, $l_z^{\nu'}=iq_\perp^{\nu'}$ and the elasto-optical tensor has been rewritten in Voight notation. Solving for the Hertz vector[31] and using $\vec{E}=\vec{\nabla}\times(\vec{\nabla}\times\vec{\pi})-\vec{P}/\epsilon_0 n_m^2$ and $\vec{H}=n_m^2\vec{\nabla}\times\dot{\vec{\pi}}/\mu_0 c^2$ to evaluate the driven fields, it can easily be shown that

$$\Delta E_x=-\frac{1}{2}\exp[i(\omega_0-\Omega)t-i(k_\parallel-q_\parallel)x]\sum_{\nu'}\frac{i(k_\parallel-q_\parallel)(\beta n_m k+iq_\perp^{*\nu'})P_z^{\nu'}-(\beta' n_m k)^2 P_x^{\nu'}}{(\beta n_m k+iq_\perp^{*\nu'})^2-(\beta' n_m k)^2}+\text{c.c.}, \quad (89)$$

$$\Delta H_y=-\frac{1}{2}\frac{ikn_m^2}{\mu_0 c}\exp[i(\omega_0-\Omega)t-i(k_\parallel-q_\parallel)x]\sum_{\nu'}\frac{i(k_\parallel-q_\parallel)P_z^{\nu'}-(\beta n_m k+iq_\perp^{*\nu'})P_x^{\nu'}}{(\beta n_m k+iq_\perp^{*\nu'})^2-(\beta' n_m k)^2}+\text{c.c.}, \quad (90)$$

$$\Delta E_y=-\frac{1}{2}n_m^2 k^2\exp[i(\omega_0-\Omega)t-i(k_\parallel-q_\parallel)x]\sum_{\nu'}\frac{P_y^{\nu'}}{(\beta n_m k+iq_\perp^{*\nu'})^2-(\beta' n_m k)^2}+\text{c.c.}, \quad (91)$$

$$\Delta H_x=-\frac{1}{2}\frac{ikn_m^2}{\mu_0 c}\exp[i(\omega_0-\Omega)t-i(k_\parallel-q_\parallel)x]\sum_{\nu'}\frac{P_y^{\nu'}(\beta n_m k+iq_\perp^{*\nu'})}{(\beta n_m k+iq_\perp^{*\nu'})^2-(\beta' n_m k)^2}+\text{c.c.} \quad (92)$$

at the surface (air side). Thus, just as in the previous sections, the calculation has been arranged to produce discontinuities in boundary conditions.

p-polarized scattered fields are obtained if ΔE_x or ΔH_y is nonzero. Solving for the boundary conditions gives

$$A_p = \frac{2i\cos\phi_0 k E_0}{(\beta + in_m\cos\phi_0)(ik_z n_m + \beta' k)} \times \sum_{\nu'} \frac{ikn_m\beta' P_x^{\nu'} - (k_{\parallel} - q_{\parallel})P_z^{\nu'}}{n_m k(\beta+\beta') + iq_\perp^{*\nu'}} . \quad (93)$$

This term cannot be simplified further but comparison with Eqs. (86)–(88) shows that only the x-z-polarized acoustical modes scatter light into this polarization. For an isotropic metal ($p_{11} = p_{12}$ and $p_{44} = 0$),

$$A_p = H_p' \frac{n_m^4}{n_m^2 - 1} p_{11} E_0 \sum_{\nu'} \frac{\Delta\rho^{*\nu'}}{(\beta+\beta')n_m k + iq_\perp^{*\nu'}} , \quad (94)$$

which is in agreement with the results for the "conductivity" calculation. As expected, this gives $p_{11} = (n_m^2 - 1)/n_m^4$.

If ΔE_y and ΔH_x are nonzero, depolarized scattering (s-polarized fields) occurs. Solving for the field amplitude gives

$$A_p = \frac{2\cos\phi_0 n_m k^2 E_0}{(i\beta' n_m k - k_z)(\beta + in_m\cos\phi_0)} \times \sum_{\nu'} \frac{P_y^{\nu'}}{(\beta+\beta')n_m k + iq_\perp^{*\nu'}} . \quad (95)$$

Inspection of Eqs. (86)–(88) shows that scattering occurs from the y-polarized modes and simplifying (95) yields

$$A_p = \frac{2\cos\phi_0 k^2 n_m^3 p_{44} E_0}{(i\beta' n_m k - ik_z)(\beta + in_m\cos\phi_0)} \times \left(\frac{\sin\phi_0(\Omega^2 - \Omega_T^2) + n_m^2 \Omega_T k v_T \beta(\beta+\beta')}{[n_m k(\beta+\beta')v_T]^2 + \Omega^2 - \Omega_T^2} \right) . \quad (96)$$

Conversion to the upshift case requires taking the complex conjugate of the acoustic parameters.

B. s-polarized incidence

This case differs from the previous one only in the form of the incident field. The components of the polarization field are

$$P_x^{\nu'} = \tfrac{1}{2} n_m^2 p_{44} A_y^{*\nu'} l_x^{*\nu'} , \quad (97)$$

$$P_y^{\nu'} = \tfrac{1}{2} n_m^2 p_{12} (A_x^{*\nu'} l_x^{*\nu'} + A_z^{*\nu'} l_z^{*\nu'}) , \quad (98)$$

$$P_z^{\nu'} = \tfrac{1}{2} n_m^2 p_{44} A_y^{*\nu'} l_z^{*\nu'} \quad (99)$$

and the field discontinuities at the boundary are given by Eqs. (89)–(92). If ΔH_x or ΔE_y are nonzero, then the s-polarized field amplitude is

$$A_p = H_s \frac{2n_m^2}{n_m^2 - 1} E_0 \sum \frac{P_y^{\nu'}}{(\beta+\beta')n_m k + iq_\perp^{*\nu'}} \quad (100)$$

and only x-z-polarized acoustical modes contribute to the scattering. Simplifying further gives for acoustically isotropic media

$$A_p = H_s \frac{n_m^4}{n_m^2 - 1} p_{12} E_0 \sum \frac{\Delta\rho^{*\nu'}}{(\beta+\beta')n_m k + iq_\perp^{*\nu'}} . \quad (101)$$

If ΔE_x or ΔH_y is nonzero, depolarized scattering from the y-polarized modes takes place with an amplitude

$$A_p = \frac{2n_m k\cos\phi_0 E_0}{(\cos\phi_0 - in_m\beta)(ik_z n_m + \beta' k)} \times \sum_{\nu'} \frac{in_m k\beta' P_x^{\nu'} - (k_{\parallel} - q_{\parallel})P_z^{\nu'}}{(\beta+\beta')n_m k + iq_\perp^{*\nu'}} . \quad (102)$$

Substituting the acoutical parameters yields

$$A_p = \frac{2n_m^3\cos\phi_0 k p_{44} E_0}{(\cos\phi_0 - in_m\beta)(in_m k_z + \beta' k)} \times \left(\frac{(k_{\parallel} - q_{\parallel})(\Omega^2 - \Omega_T^2) - n_m^2 k^2 \Omega_T v_T \beta'(\beta+\beta')}{[n_m k(\beta+\beta')v_T]^2 + \Omega^2 - \Omega_T^2} \right) . \quad (103)$$

IX. BRILLOUIN SPECTRUM

The frequency spectrum of the scattered light is calculated by first evaluating the Brillouin spectrum from a single acoustical mode and then summing over all of the possible phonon states. For a given mode μ the scattered field at the observation point described by $\vec{R}$ is written

$$\vec{E}^{\mu}(\vec{R}, t) = \tfrac{1}{2} E_0 u_0^{\mu} \exp\{[(\omega_0 \pm \Omega)t - (k_{\parallel} \pm q_{\parallel})x + k_z z]\} \times \left| \sum_p \vec{F}^p \right| \quad (104)$$

where the summation over p includes all of the scattering mechanisms. For example,

$$\sum_p \vec{F}^p = \hat{j}\, \frac{(A_c + A_p)}{E_0}$$

for the polarized scattering of s-polarized incident light by the corrugation and elastooptic effects. The frequency spectrum is given by

$$S^{\mu}(\vec{R}, \omega') = \frac{1}{2\pi} \int \langle \vec{E}^{\mu}(t+\tau) \cdot \vec{E}^{*\mu}(t) \rangle e^{i\omega'\tau} d\tau + \text{c.c.} , \quad (105)$$

where ω' is the frequency of the scattered light. Assuming that the damping of the μth mode is of the form $e^{-\Gamma\mu t}$, the spectral density $S(\vec{R}, \omega')$ is calculated to be

$$S^{\mu}(\vec{R},\omega')=\frac{1}{2}\langle|u_0^{\mu}|^2\rangle\frac{\Gamma^{\mu}/\pi}{(\omega'-\omega_0\mp\Omega)^2+\Gamma^{\mu 2}}S_0\times\sum_{p}\sum_{p'}\vec{F}^{p}\cdot\vec{F}^{*p'}, \qquad (106)$$

with $S_0=\frac{1}{2}|E_0|^2$. The total frequency spectrum is a summation over all the acoustical modes which contribute to the scattering, i.e.,

$$S(\vec{R},\omega')=\sum_{\mu}[S_s^{\mu}(\vec{R},\omega')+S_a^{\mu}(\vec{R},\omega')], \qquad (107)$$

where s and a refer to the symmetric and antisymmetric modes. For free-standing thin films such that $2q_{\perp}L_z\gg 1$ is not satisfied, this summation must be done term by term. If $2q_{\perp}L_z\gg 1$, the summations are replaced by integrals over $\vec{q}$ space the details of which depend on the acoustical modes.

A. Liquids

The appropriate density of states for a liquid was discussed previously in Sec. III. The spectral density is given by

$$\sum_{\mu}S_a^{\mu}(\vec{R},\omega')=\sum_{\mu}S_s^{\mu}(\vec{R},\omega')=\frac{2V}{(2\pi)^3}S_0\int\int\langle|u_0^{\mu}|^2\rangle\frac{\Gamma^{\mu}/\pi}{(\omega'-\omega_0\mp\Omega)^2+\Gamma^{\mu 2}}\sum_{p}\sum_{p'}\vec{F}^{p}\cdot\vec{F}^{*p'}\frac{\Omega}{v_L(\Omega^2-\Omega_L^2)^{1/2}}d\Omega\,|d\vec{q}_{\parallel}| \qquad (108)$$

for both the symmetric and antisymmetric modes. For small solid angles $\Delta\Omega_s$ subtended at the detector,

$$\int|d\vec{q}_{\parallel}|\to|d\vec{q}_{\parallel}|=k^2\cos\phi_s\Delta\Omega_s$$

(Ref. 32). If the "skin depth" of the incident light is no more than a few optical wavelengths then all of the terms inside the integral, except the Lorentzians, have broad frequency distributions. Since $\Omega\gg\Gamma^{\mu}$, the Lorentzian is effectively a δ function, i.e.,

$$\frac{\Gamma^{\mu}/\pi}{(\omega'-\omega_0\mp\Omega)^2+\Gamma^{\mu 2}}\to\delta(\omega'-\omega_0\mp\Omega). \qquad (109)$$

Evaluating the integral over Ω yields

$$S(\vec{R},\omega')=S_a(\vec{R},\omega')+S_s(\vec{R},\omega')=\frac{K_BTk^2\cos\phi_s\Delta\Omega_sS_0}{(2\pi)^3\rho\Omega v_L(\Omega^2-\Omega_L^2)^{1/2}}\times\sum_{p}\sum_{p'}\vec{F}^{p}\cdot\vec{F}^{*p'}, \qquad (110)$$

which relates the spectral distribution of the scattered Poynting vector to the magnitude of the incident optical power per unit area. In an actual experiment the incident light illuminates a finite area of the sample surface so that

$$I(\vec{R},\omega')/I_0=\cos\phi_sS(\vec{R},\omega')/\cos\phi_0S_0$$

for the ratio of the total detected scattered light $I(\vec{R},\omega')$ to the incident light power I_0. Therefore

$$\frac{I(\vec{R},\omega')}{I_0\Delta\Omega_s}=\frac{k^2\cos^2\phi_sK_BT}{(2\pi)^3\rho\Omega v_L(\Omega^2-\Omega_L^2)^{1/2}\cos\phi_0}\times\sum_{p}\sum_{p'}\vec{F}^{p}\cdot\vec{F}^{*p'} \qquad (111)$$

is the final result for frequencies $\omega'=\omega_0\pm\Omega$. Finally we note that for penetration depths of the incident field of many wavelengths, the integral in Eq. (108) must be evaluated explicitly and the δ-function approximation for the Lorentzian terms is not valid.

B. Solids

Consider first the case of y-polarized shear modes. The treatment is exactly the same as for the liquid case and the result is

$$\frac{I(\vec{R},\omega')}{I_0\Delta\Omega_s}=\frac{k^2\cos^2\phi_sK_BT|A_p|^2}{(2\pi)^3\rho\Omega v_T(\Omega^2-\Omega_T^2)^{1/2}\cos\phi_0} \qquad (112)$$

with A_p given by Eq. (96) or (103) for p- and s-polarized incident light, respectively.

The analysis for the x-z-polarized acoustical modes is also the same as for liquids. In region I $(\Omega>\Omega_L)$

$$\frac{I(\vec{R},\omega')}{I_0\Delta\Omega_s}=\frac{k^2\cos^2\phi_sK_BT}{\rho\Omega(2\pi)^3\cos\phi_0}\frac{v_L(\Omega^2-\Omega_L^2)^{1/2}+v_T(\Omega^2-\Omega_T^2)^{1/2}}{v_L(\Omega^2-\Omega_L^2)^{1/2}v_T(\Omega^2-\Omega_T^2)^{1/2}}\sum_{p}\sum_{p'}\left(\frac{\vec{F}_s^{p}\cdot\vec{F}_s^{*p'}}{\sum_{\nu'}|\vec{A}_s^{\nu'}|^2}+\frac{\vec{F}_a^{p}\cdot\vec{F}_a^{*p'}}{\sum_{\nu'}|\vec{A}_a^{\nu'}|^3}\right). \qquad (113)$$

For region II $(\Omega_L>\Omega>\Omega_T)$ the modes are degenerate and

$$\frac{I(\vec{R},\omega')}{I_0\Delta\Omega_s}=\frac{k^2\cos^2\phi_sK_BT}{\rho\Omega(2\pi)^3\cos\phi_0v_T(\Omega^2-\Omega_T^2)^{1/2}}\sum_{p}\sum_{p'}\vec{F}^{p}\cdot\vec{F}^{*p'}. \qquad (114)$$

Finally, since scattering from surface phonons occurs from only one value of $\vec{q}_{\parallel}$ for a given scattering geometry, the scattered spectrum consists of two discrete Lorentzians with

$$\frac{I(\vec{R},\omega')}{I_0\Delta\Omega_s}=\frac{k^2\cos^2\phi_s K_B T}{(2\pi)^2\cos\phi_0\rho v_R\Omega_R\sum_{\nu'}\sum_{\eta'}[A_i^{\nu'}A_i^{*\eta'}/(\alpha^{\nu'}+\alpha^{*\eta'})]}\;\frac{\Gamma^{\mu}/\pi}{(\omega'-\omega_0\mp\Omega)^2+\Gamma^{\mu 2}}\sum_{p}\sum_{p'}\vec{F}^{p}\cdot\vec{F}^{*p'}. \tag{115}$$

The spectra described by Eqs. (111)–(114) have a number of interesting features. We note that both the volume and area cancel out, as expected on physical grounds, so that the frequency spectra are essentially independent of sample size. For small penetration depths of the incident light into the opaque medium, all of the spectral features for $\Omega > \Omega_T$ are relatively broad. The only well-defined feature is due to scattering from thermal surface phonons. As the penetration depth increases, the frequency spectrum undergoes a transition for $\Omega > \Omega_T$ to the usual spectrum associated with Brillouin scattering from "infinite" media.[1-6]

Finally we comment on the apparent discontinuities which are predicted by Eqs. (111)–(114) for $\Omega \simeq \Omega_T$ and $\Omega \simeq \Omega_L$. In many of these cases there are compensating terms contained in $\vec{F}^p$ and in the final expressions no discontinuities are predicted (see Sec. X). Furthermore in these regions the replacement of the Lorentzian terms by δ functions is invalid and equations of the type given by (108) must be evaluated in detail. This results in finite peaks with widths of the order Γ^{μ}.

X. METALS

In this section the formalism outlined to this point is applied to Brillouin scattering from metals in order to compare with recently reported experimental spectra.[8,9] The elasto-optical effect is treated here in terms of conductivity fluctuations. For all the cases considered, no depolarized scattering is predicted, or observed.[8,9]

A. Liquid metals

Consider first the case of s-polarized incidence. Substituting Eqs. (57)–(59), (76), and (77) into (111) yields

$$\frac{I(\vec{R},\omega')}{I_0\Delta\Omega_s}=\frac{4k^4\cos\phi_0\cos^2\phi_s|n_m^2-1|^2K_BT(\Omega^2-\Omega_L^2)^{1/2}}{|(\cos\phi_0-in_m\beta)(i\beta'n_m-\cos\phi_s)|^2(2\pi)^3\rho v_L\Omega^3}\left|1-\frac{\Omega^2}{[n_m(\beta+\beta')kv_L]^2+\Omega^2-\Omega_L^2}\right|^2 \tag{116}$$

for $\Omega > \Omega_L$ and $I(\vec{R},\omega')/I_0\Delta\Omega_s=0$ for $\Omega_L > \Omega$. The spectrum starts from zero at $\Omega=\Omega_L$ (corresponding to scattering from sound waves traveling parallel to the surface) and peaks at $\Omega \sim 1.22\,\Omega_L$. The first term originates from the corrugation effect and the second is due to acoustically induced changes in the local conductivity. In the vicinity of $\Omega\sim\Omega_L$ the ratio of the conductivity to corrugation effects is $1/2n_m^2$ which is small for a good metal. Therefore the corrugation effect is the dominant scattering mechanism and the conductivity contribution is only a few percent. The spectrum can be further simplified to give

$$I(\vec{R},\omega')/I_0\Delta\Omega_s=4k^4\cos\phi_0\cos^2\phi_s K_BT(\Omega^2-\Omega_L^2)^{1/2}/(2\pi)^3\rho v_L\Omega^3 \tag{117}$$

for a highly reflecting metal characterized by $|n_m|^2 \gg 1$.

The frequency spectrum for p-polarized incidence is calculated from Eqs. (52), (53), (59), (72), (73), (77), and (111). The result is

$$\frac{I(\vec{R},\omega')}{I_0\Delta\Omega_s}=\frac{4k^4\cos\phi_0\cos^2\phi_s|n_m^2-1|^2K_BT(\Omega^2-\Omega_L^2)^{1/2}}{|(in_m\cos\phi_s+\beta')(\beta+in_m\cos\phi_0)|^2(2\pi)^3\rho v_L\Omega^3}\left|X-\frac{Y\Omega^2}{[n_mk(\beta+\beta')v_L]^2+\Omega^2-\Omega_L^2}\right|^2, \tag{118}$$

with

$$X=\beta\beta'+\sin\phi_0\sin\phi_s \quad\text{and}\quad Y=\beta\beta'+\sin\phi_0\sin\phi_s/n_m^2.$$

In the vicinity of $\Omega\sim\Omega_L$ the frequency spectrum is similar to that for the s-polarized incidence case and the previous comments regarding structure and relative contributions are valid here also. In the limit of a good metal, i.e., $|n_m\cos\phi_s|^2\gg 1$ and $|n_m\cos\phi_0|^2\gg 1$,

$$I(\vec{R},\omega')/I_0\Delta\Omega_s=4k^4(1-\sin\phi_s\sin\phi_0)K_BT(\Omega^2-\Omega_L^2)^{1/2}/(2\pi)^3\rho v_L\cos\phi_0\Omega^3\,. \tag{119}$$

Note that the frequency spectrum is exactly the same as for s-polarized incidence in this limit but the scattering intensities are different.

Experiments have been performed by Dil and Brody[8] on the metallic liquids gallium and mercury. Based on the parameters given in their paper Eq. (117) [or (119)] was evaluated for the spectrum which exhibited the best signal-to-noise characteristics, that for liquid gallium. As shown in Fig. 4, the agreement between experiment and theory is excellent.

B. Solid metals

Consider first the Brillouin spectrum in region I defined by $\Omega > \Omega_L$. The spectrum evaluated from the equations in the previous sections is

$$\frac{I_s(\vec{R},\omega')}{I_0\Delta\Omega_s} = H\,\frac{8k^2\cos^3\phi_s K_B T \Omega\Omega_T^4(\Omega^2-\Omega_T^2)^{1/2}[v_L(\Omega^2-\Omega_L^2)^{1/2}+v_T(\Omega^2-\Omega_T^2)^{1/2}]}{(2\pi)^3\rho v_L v_T\cos\phi_0(\Omega^2-\Omega_L^2)^{1/2}[\Omega_L^2(\Omega^2-2\Omega_T^2)^2+4\Omega_T^4(\Omega^2-\Omega_T^2)]}\;\frac{|v_L n_m k(\beta+\beta')|^2}{|[v_L n_m k(\beta+\beta')]^2+\Omega^2-\Omega_L^2|^2}\,, \tag{120}$$

where H is either H_s or H_p' depending on whether the incident light is s or p polarized. For the antisymmetric mode

$$\frac{I_a(\vec{R},\omega')}{I_0\Delta\Omega_s} = \frac{k^2\cos^2\phi_s K_B T \Omega(\Omega^2-\Omega_L^2)^{1/2}[v_L(\Omega^2-\Omega_L^2)^{1/2}+v_T(\Omega^2-\Omega_T^2)^{1/2}]}{(2\pi)^3\rho v_L v_T\cos\phi_0(\Omega^2-\Omega_T^2)^{1/2}[2\Omega_T^2(\Omega^2-\Omega_L^2)+(2\Omega_T^2-\Omega^2)^2]}\left|H+H'\,\frac{2\Omega_T^2-\Omega^2}{[v_L n_m k(\beta+\beta')]^2+\Omega^2-\Omega_L^2}\right|^2 \tag{121}$$

with $H=H'=H_s$ for s-polarized incident light, and $H=H_p$ and $H'=H_p'$ for the p-polarized case. The Brillouin spectrum is the sum of the two, i.e.,

$$I(\vec{R},\omega')/I_0\Delta\Omega_s = [I_a(\vec{R},\omega')+I_s(\vec{R},\omega')]/I_0\Delta\Omega_s\,. \tag{122}$$

The symmetric mode spectrum arises solely from conductivity fluctuations whereas both corrugation (first term) and elasto-optical (second term) mechanisms contribute to the scattering from the antisymmetric sound waves. The ratio of the conductivity to corrugation terms is of the order $1/n_m^2$ and for metals with $|n_m| \sim 5-10$ this constitutes only a few percent. For $|n_m|^2 \gg 1$,

$$\frac{I(\vec{R},\omega')}{I_0\Delta\Omega_s} = \frac{k^4 K_B T\cos\phi_0\cos\phi_s\Omega(\Omega^2-\Omega_L^2)^{1/2}[v_L(\Omega^2-\Omega_L^2)^{1/2}+v_T(\Omega^2-\Omega_T^2)^{1/2}]}{(2\pi)^3\rho v_L v_T(\Omega^2-\Omega_T^2)^{1/2}[2\Omega_T^2(\Omega^2-\Omega_L^2)+(2\Omega_T^2-\Omega^2)^2]} \tag{123}$$

and

$$\frac{I(\vec{R},\omega')}{I_0\Delta\Omega_s} = \frac{k^4 K_B T(1-\sin\phi_0\sin\phi_s)\Omega(\Omega^2-\Omega_L^2)^{1/2}[v_L(\Omega^2-\Omega_L^2)^{1/2}+v_T(\Omega^2-\Omega_T^2)^{1/2}]}{(2\pi)^3\cos\phi_0\rho v_L v_T(\Omega^2-\Omega_T^2)^{1/2}} \tag{124}$$

for s- and p-polarized incident light, respectively. These two spectra are identical in structure but do differ in intensity.

The frequency spectrum in region II ($\Omega_L > \Omega > \Omega_T$) is calculated in the same way as discussed previously. Here

$$\frac{I(\vec{R},\omega')}{I_0\Delta\Omega_s} = \frac{16k^2\cos^2\phi_s K_B T\Omega\Omega_T^4(\Omega^2-\Omega_T^2)^{1/2}}{(2\pi)^3\cos\phi_0\rho v_T[(2\Omega_T^2-\Omega^2)^4+16\gamma^2\Omega_T^6(\Omega^2-\Omega_T^2)]}\left|\gamma H-\frac{H'(2\Omega_T^2-\Omega^2)}{\Omega_L[v_L n_m k(\beta+\beta')+\gamma\Omega_L]}\right|^2, \tag{125}$$

with $\gamma=(1-\Omega^2/\Omega_L^2)^{1/2}$, $H=H'=H_s$ for s-polarized incidence, and $H=H_p$ and $H'=H_p'$ if the incident light is p polarized. The corrugation terms are dominant for a good metal and the spectrum has minima at Ω_T and Ω_L. However the ratio of the conductivity to corrugation terms $[(2\Omega_T^2-\Omega^2)/\Omega_L^2 n_m\gamma]$ is not negligible for metals with $|n_m|$ in the range 5–10 (unless $\Omega^2 \sim 2\Omega_T^2$).

Scattering from surface phonons is characterized by two Lorentzians centered at $\omega'=\omega_0 \pm \Omega_R$. The spectrum is given by

$$\frac{I(\vec{R},\omega')}{I_0\Delta\Omega_s} = \frac{k^2\cos\phi_s K_B T}{(2\pi)^2\rho v_R\Omega_R\sum_{\nu'}\sum_{\eta'}(A_i^{\nu'}A_i^{*\eta'}/\alpha^{\nu'}+\alpha^{*\eta'})}\;\frac{\Gamma^{\mu}/\pi}{(\omega'-\omega_0\mp\Omega)^2+\Gamma^{\mu 2}}$$
$$\times\left|H\alpha^{(2)}\left(1-\frac{1}{(\alpha^{(1)}\alpha^{(2)})^{1/2}}\right)+H'\,\frac{\Omega_R^3/\Omega_L^2}{n_m k(\beta+\beta')v_R+\Omega_R(1-\Omega_R^2/\Omega_L^2)^{1/2}}\right|^2. \tag{126}$$

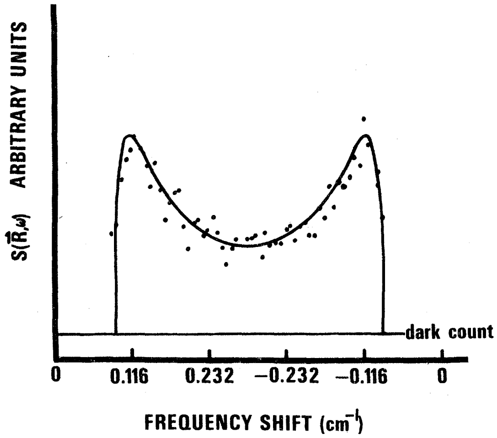

FIG. 4. Experimental and theoretical (solid line) Brillouin spectrum from liquid gallium. These data were supplied by Brody.

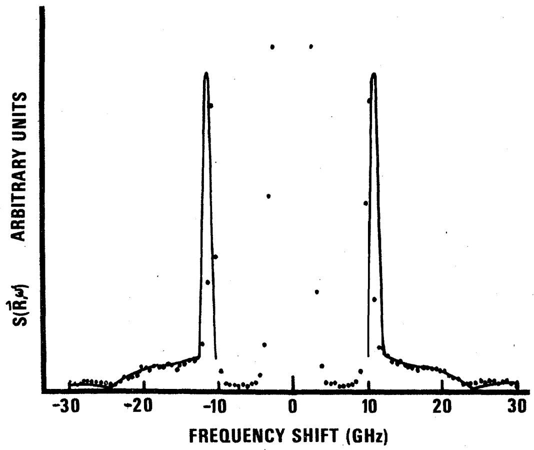

FIG. 5. Experimental and theoretical (solid line) Brillouin spectrum from isotropic aluminum.

and the previous comments about H and H' are applicable here. For this case the contribution from the conductivity term is small, but not negligible (~5%).

Brillouin scattering from isotropic metals has been reported by Sandercock[9] and a comparison with his results for isotropic aluminum is shown in Fig. 5. Scattering from both the corrugation and conductivity mechanisms was included in the calculation and the refractive-index data was taken from Ref. 33. The instrumental profile was estimated from the published curve[9] and it was assumed that the instrumental width was much greater than Γ^u for the surface phonons. The difference in the observed and calculated positions of the spectral lines originating from scattering by surface waves is attributed to a difference between the elastic constants of this sample and those reported previously.[24] Nevertheless the agreement between the experimental and theoretical frequency spectra is excellent. The absolute scattering intensity was also estimated from the experimental parameters[34] and by modelling the instrumental line as a rectangular profile. A value of 35 counts/(sec incident-mW sr) was obtained which compares favourably with the experimental value of 22 in the same units.

XI. SUMMARY

In this paper we have outlined a total field approach to the analysis of light scattering by sound waves at the surfaces of opaque materials. The acoustical modes used are those appropriate to stress-free boundary conditions and the scattering was analyzed in terms of both the corrugation and electro-optical effects.

The acoustical modes were found to be linear superpositions of standing waves of the phonons of an infinite medium, i.e., the shear and longitudinal waves. In a liquid, only standing-wave longitudinal modes occur. The case of a solid is more complicated and three separate acoustical frequency regimes have been considered. These regions are $\Omega > \Omega_L$, $\Omega_L > \Omega > \Omega_T$, and $\Omega = \Omega_R$. One mode consists of a y-polarized standing-wave shear which exists for $\Omega > \Omega_T$. The other two modes are polarized in a plane normal to the surface and consist of standing-wave shear and longitudinal waves for $\Omega > \Omega_L$, of a standing-wave shear and evanescent longitudinal modes at both surfaces for $\Omega_L > \Omega > \Omega_T$ and of a surface phonon with both evanescent shear and longitudinal waves at $\Omega = \Omega_R$.

Basically two scattering mechanisms were considered, i.e., corrugation scattering and elasto-optical scattering. Sound waves produce a surface corrugation which scatters light in a way reminiscent of a traveling diffraction grating. This mechanism was found to be responsible for the Brillouin spectrum of highly reflecting liquid and solid metals. The elasto-optical effect within the "skin depth" of the material was also analyzed for the general case. Treated as a special case of the elasto-optical effect were conductivity fluctuations in "good" metals. The good agreement between the present theory and the experimental results of Dil and Brody[8] and Sandercock[9] is considered to be a verification of this formalism for corrugation scattering.

This theory has also been used previously[11,12] to analyze Brillouin scattering in thin films deposited on substrates. In that case the elasto-optical effect was the dominant mechanism and the corrugation effect contributed of the order of 10%. The agreement with experiment was excellent[12] for that case also which indicates that the present formulation is also correct for the elasto-optical mechanism.

In summary, it appears that Brillouin scattering at the surfaces of opaque materials is well understood and that experimental results can now be used to obtain information about sound waves at surfaces.

ACKNOWLEDGMENTS

The authors wish to thank Dr. E. Brody and Dr. J. Sandercock for many fruitful discussions, critical comments, and for making their data available. Research supported by the Canadian National Research Council.

APPENDIX

In this Appendix we investigate the effects of fluid shear viscosity on the longitudinal standing-wave modes in a liquid. The incident and reflected longitudinal fields are given by Eq. (4) and substituting into Eq. (3) yields

$$T_{zx} = -u_0^\mu \Omega\eta \frac{q_\parallel q_\perp}{q}(1-\Gamma)e^{i(\Omega t - q_\parallel x)} + \text{c.c.}, \tag{A1}$$

$$T_{zz} = -i\,\frac{u_0^\mu}{2}(\rho v_L^2 + 2i\Omega\eta)\frac{q_\perp^2}{q}(1+\Gamma)e^{i(\Omega t - q_\parallel x)} + \text{c.c.}$$

at $z=0$. It is impossible to satisfy both $T_{zx}=0$ and $T_{zz}=0$ with a single choice of Γ.

It is therefore necessary to consider additional modes, in this case an evanescent shear wave at the surface. The fields are of the form

$$u_i = \tfrac{1}{2}u_0^\mu K_i e^{i(\Omega t - q_\parallel x) - bz} + \text{c.c.}, \tag{A2}$$

with the real part of b chosen positive to produce evanescent waves. Requiring $\vec{\nabla}\cdot\vec{u}=0$ (for a shear mode) gives $K_x = (ib/q_\parallel)K_z$. The stresses are

$$T_{xz} = T_{zx} = \tfrac{1}{2}u_0^\mu i\Omega\eta(-iq_\parallel K_z - bK_x) \times e^{i(\Omega t - q_\parallel x) - bz} + \text{c.c.}, \tag{A3}$$

$$T_{xx} = u_0^\mu \Omega\eta q_\parallel K_x e^{i(\Omega t - q_\parallel x) - bz} + \text{c.c.}, \tag{A4}$$

and

$$T_{zz} = -u_0^\mu i\Omega\eta b K_z e^{i(\Omega t - q_\parallel x) - bz} + \text{c.c.} \tag{A5}$$

Solving the force-balance equation ($\nabla_i T_{ij} = \rho \ddot{u}_j$) gives

$$b^2 = i(\rho\Omega/\eta)(1 + q_\parallel^2\eta/i\rho\Omega). \tag{A6}$$

For the liquids of Ref. 8, the second term is typically less than 10^{-2} and can be neglected. Thus

$$b = (\rho\Omega/2\eta)^{1/2}(1+i). \tag{A7}$$

This shear mode can now be used to satisfy both stress-free boundary conditions. The contributions to the surface stresses are

$$T_{zx} = \frac{1}{2}u_0^\mu \frac{\Omega\eta}{q_\parallel}(b^2 + q_\parallel^2)K_z e^{i(\Omega t - q_\parallel x)} + \text{c.c.} \tag{A8}$$

and

$$T_{zz} = u_0^\mu i b\Omega\eta K_z e^{i(\Omega t - q_\parallel x)} + \text{c.c.} \tag{A9}$$

We note that $b^2 \gg q_\parallel^2$ for the shear mode with the result that $T_{zx} \gg T_{zz}$. Furthermore, since $T_{zz} \gg T_{zx}$ for the longitudinal waves, the shear modes are neglected in satisfying $T_{zz}=0$, i.e., $\Gamma = -1$ and both terms are used in ensuring that $T_{zx}=0$. This yields

$$K_z = -(2q_\perp/q)(2iq_\parallel^2\eta/\rho\Omega) \tag{A10}$$

and

$$K_x = (4q_\perp/q)(q_\parallel^2\eta/2\rho\Omega)^{1/2}(1+i). \tag{A11}$$

We now estimate the effect of this shear mode on the scattered fields. It is easy to show that for the total corrugation

$$\delta = -2\,\frac{(\Omega^2 - \Omega_L^2)^{1/2}}{\Omega}\left(1 + \frac{2iq_\parallel^2\eta}{\rho\Omega}\right). \tag{A12}$$

The second term is attributed to the shear mode and can be neglected for phonons in the gigahertz frequency range. Since $\vec{\nabla}\cdot\vec{u}=0$ for the shear mode, there is no contribution to the elasto-optical effect. Therefore the effect of this evanescent mode on the Brillouin spectrum is negligible.

[1]P. A. Fleury, in *Physical Acoustics*, edited by W. P. Mason and R. N. Thurston (Academic, New York, 1970), Vol. VI, p. 1.
[2]J. R. Sandercock, in *Advances in Solid State Physics*, edited by H. J. Queisser (Pergamon, Braunschweig, 1975), Vol. XV, p. 183.
[3]G. B. Benedek and K. Fritsch, Phys. Rev. 149, 647 (1966).
[4]G. I. Stegeman and B. P. Stoicheff, Phys. Rev. A 7, 1160 (1973).
[5]H. Kiefte and M. J. Clouter, J. Chem. Phys. 64, 1816 (1976).
[6]R. G. Ulbrich and C. Weisbuch, Phys. Rev. Lett. 38, 865 (1977).
[7]J. R. Sandercock, Phys. Rev. Lett. 28, 237 (1972).
[8]J. G. Dil and E. M. Brody, Phys. Rev. B 14, 5218 (1976).
[9]J. R. Sandercock, Solid State Commun. 26, 547 (1978).
[10]J. R. Sandercock, Phys. Rev. Lett. 29, 1735 (1972).
[11]N. L. Rowell, V. So, and G. Stegeman, Annual Conference of the Canadian Association of Physicists, Québec, 1976 (unpublished).

[12]N. L. Rowell, V. So, and G. I. Stegeman, Appl. Phys. Lett. 32, 154 (1978).

[13]B. I. Bennett, A. A. Maradudin, and L. R. Swanson, in *Proceedings of the Second International Conference on Light Scattering in Solids*, edited by M. Balanski (Flammarion, Paris, 1971), p. 443; Ann. Phys. (Paris) 71, 357 (1972).

[14]A. Dervisch and R. Loudon, J. Phys. C 9, L669 (1976).

[15]G. Dresselhaus and A. S. Pine, Solid State Commun. 16, 1001 (1975).

[16]R. Loudon, Phys. Rev. Lett. 40, 581 (1978).

[17]N. L. Rowell and G. I. Stegeman, Solid State Commun. (to be published).

[18]R. Loudon, J. Phys. C 11, 403 (1977).

[19]L. Bergman, *Ultrasonics* (Bell, London, 1938), p. 164.

[20]G. I. Stegeman, IEEE Trans. Son. Ultrasonics 23, 33 (1976).

[21]A. Madeyski and L. W. Kessler, IEEE Trans. Son. Ultrasonics 23, 363 (1976).

[22]S. Mishra and R. Bray, Phys. Rev. Lett. 39, 222 (1977).

[23]G. I. Stegeman, J. Appl. Phys. (to be published).

[24]B. A. Auld, *Acoustic Waves and Fields in Solids* (Wiley, New York, 1973), Vols. I and II.

[25]M. Dupuis, R. Mazo, and L. Onsager, J. Chem. Phys. 33, 1452 (1960).

[26]R. Stratton, Philos. Mag. 44, 519 (1953).

[27]G. W. Farnell, in Ref. 1, p. 109.

[28]W. G. Mayer, G. B. Lamers, and D. C. Auth, J. Acoust. Soc. Am. 42, 1255 (1967).

[29]E. G. Lean, in *Progress in Optics*, edited by E. Wolf (North-Holland, Amsterdam, 1973), Vol. II, p. 124.

[30]T. C. Padmore and G. I. Stegeman, J. Appl. Phys. 47, 1209 (1976).

[31]J. A. Stratton, *Electromagnetic Theory* (McGraw-Hill, New York, 1941).

[32]D. L. Mills, A. A. Maradudin, and E. Burstein, Ann. Phys. (N.Y.) 56, 504 (1970).

[33]G. Hass, *American Institute of Physics Handbook*, 3rd ed. (McGraw-Hill, New York, 1972).

[34]J. R. Sandercock (private communication).